HAL
open science

Asymptotic analysis of Painlevé' s paradox

Zhen Zhao, Caishan Liu, Chen Bin, Bernard Brogliato

To cite this version:

Zhen Zhao, Caishan Liu, Chen Bin, Bernard Brogliato. Asymptotic analysis of Painlevé' s paradox. Multibody System Dynamics, 2015, 35 (3), pp.299-319. 10.1007/s11044-014-9448-1 . hal-01232780

HAL Id: hal-01232780

https://inria.hal.science/hal-01232780

Submitted on 3 Nov 2017

HAL is a multi-disciplinary open access archive for the deposit and dissemination of scientific research documents, whether they are published or not. The documents may come from teaching and research institutions in France or abroad, or from public or private research centers.

L'archive ouverte pluridisciplinaire **HAL**, est destinée au dépôt et à la diffusion de documents scientifiques de niveau recherche, publiés ou non, émanant des établissements d'enseignement et de recherche français ou étrangers, des laboratoires publics ou privés.

Asymptotic analysis of Painlevé's paradox

Zhen Zhao[1] · Caishan Liu[2] · Bin Chen[2] · Bernard Brogliato[3]

Abstract Painlevé's paradox is a well-known problem in rigid-body dynamics, of which the forward dynamics equations could have no solution. To handle this situation, an assumption of *tangential impact* is often introduced. Although the assumption seems to provide a good fix, it still needs to be mathematically examined via analyzing the asymptotic property of a compliance-based model at the limit of rigidity. In this paper, we revisit the paradox using the typical Painlevé's example of a rod sliding on a rough surface. For convenience, the interaction at the contact point of the rod is represented by a linear spring to scale the local normal compliance, coupled with Coulomb's law to reflect friction. We perform an asymptotic analysis using the spring stiffness as a perturbation parameter. The rod dynamics in the Painlevé's paradox, accompanying the variation of friction status, consists of three distinct phases as follows: An initial period of sliding which allows contact force to diverge with the increase of the spring stiffness, a period of sticking which ends at the occurrence of a reverse slip motion, and a reverse slip phase which causes the rod to be detached from the contact surface. As the stiffness goes to infinity, all the time intervals of the three phases converge to zero. This analysis theoretically confirms the assumption of the *tangential impact* in the paradox of sliding rod dynamics.

Keywords Painlevé paradox · Coulomb's friction · Singularity

C. Liu
liucs@pku.edu.cn

Z. Zhao
bhzhaozhen@buaa.edu.cn

B. Brogliato
bernard.brogliato@inria.fr

1 School of Aeronautic Science and Engineering, Beihang University, Beijing 100191, China

2 State Key Laboratory for Turbulence and Complex Systems, College of Engineering, Peking University, Beijing 100871, China

3 Bipop Team-Project, INRIA, ZIRST Montbonnot, 655 Avenue de I'Europe, 38334 Saint-Ismier, France

1 Introduction

Painlevé paradox occurs in rigid-body dynamics of contact with friction, where the instantaneous solutions of the contact forces may become *inconsistent* or *indeterminate* as constraints are adopted to describe the normal interaction at contacts. This problem was first recognized by Painlevé [1] in studying a rigid rod or rectangular block sliding on a rough plane. The paradox challenges the ability of rigid-body models in predicting the actual motion of mechanical systems, thus it stands for a fundamental problem in rigid-body dynamics [2–5].

Since Painlevé's work, results on the problem have been reported in a tremendous amount of literature; see, e.g., [4, 5], and references cited therein. In this paper, we focus on the paradox in the *inconsistent* mode, namely, the solutions of the contact forces are nonexistent. To eliminate the paradox, Lecornu [6] first noticed that the rigid body assumption should be relaxed. In other words, the constraint in modeling the point-contact interaction should be replaced by a compliance-based model with a constitutive relationship to determine the contact force [7–11]. Indeed, the numerical simulations via a compliance-based model, as have been demonstrated in [12, 13], yield no paradox.[1]

Nevertheless, central to the Painlevé paradox is the question of why a completely rigid-body model can work well in some cases, yet it is invalid when the system changes its configuration into a specific range. With respect to the consideration, many authors attributed the Painlevé's paradox to a specific singularity inherent in rigid-body dynamics [17–22]. This singularity is basically due to unilateral constraints whose property may vary with the evolutions of friction and/or the configuration of the system.

To explicitly expose the singularity in a rigid-body model, Lötstedt [3] developed a uniform LCP-based method via the complementarity condition that should be satisfied by unilateral constraints. This method was then extended into multibody systems by Pfeiffer and Glocker [23], and followed by many authors [24–27] with modifications in numerical implementation. Based on an LCP-based method, the singularity can be easily identified according to system configurations and friction state on the contact surface. Besides the widely studied Painlevé's example [18, 28], recent studies have revealed that many mechanical systems are intervened by the singularity. Examples are a robot system on a moving belt [28–30], an IPOS-like mechanism [31], and the passive walking systems [32].

In order to understand what happens as the singularity occurs, Génot and Brogliato [18] performed a theoretical analysis for the forward dynamics of a sliding rough rod described by a fully rigid-body model. By setting its motion to begin with consistent slippage, they analyzed the local property of the dynamics around the singular points, and proved that the slip motion must cease prior to the arrival of the singularity. Namely, the singularity is inaccessible as the forward dynamics starts in a consistent state. Following the work in [18], Nordmark et al. [33] concluded that the ambiguity of the Painlevé's paradox in the case of inconsistent solution is automatically resolved by eliminating the possibility of reaching such a condition. This conclusion is basically true if friction is uniform on the whole contact surface and the rod motion is initialized with consistent slippage. Namely, the coefficient of friction takes a fixed value during the sliding motion. However, as the value of coefficient

[1] It is worth noting that the stick–slip transition in friction must be correctly distinguished in a compliance-based model [12, 13]. Otherwise, an unrealistic solution with inconsistent energy, as was discovered in frictional impact [14], will appear. Also, replacing the Coulomb law for the dry friction by a modified version without stick status, as has been done in [15] for the purpose of eliminating the paradox, does not agree with the essence of dry friction according to the recent development [16].

of friction changes, or a contact is initialized with an initial condition in a singular configuration, the singularity cannot be eliminated from the fully rigid-body models of practical systems.

Of course, real mechanical systems reject any singularity, so that its occurrence in a mathematical model is usually related to a specific physical phenomenon that requires a new physical law for characterization. For the inconsistent case of Painlevé's paradox, it has been shown that a consistent solution can be obtained under an impact assumption [34, 35], which historically was termed tangential impact [36], or impact without collision [18], or dynamic jamming [31]. The impact assumption has been supported by the numerical investigations fulfilled under a variety of compliance-based models [12, 13]. In addition, experimental investigations [28] also showed that the unstable phenomenon of a robotic system touching a moving belt essentially originated from an event of a tangential impact.

Although all the numerical and experimental phenomena seem to support that the Painlevé paradox in the inconsistent mode corresponds to an impact process, to the best of our knowledge, an asymptotic analysis by analyzing a compliance-based model following the limit of rigidity is still absent. Dupont and Yamajako [8] and Song et al. [10] adopted a singular perturbation technique to justify the rationality of rigid-body dynamics in the regular cases. According to their analysis, the solution of the full-order model with contact compliance can converge to the one of reduced-order-rigid-body model if and only if the dynamics of the elastic boundary layer around a contact point is exponentially stable. Nevertheless, for the reduced-order-rigid-body model in the Painlevé paradox, the singular perturbation analysis only reveals that the boundary layer is unstable, yet it tells us nothing of what happens.

We notice that Le Suan [37] has performed an asymptotic analysis for the inconsistent mode appearing in a Painlevé–Klein system, and proved that the inconsistency would be engaged into a shock with the divergence of the contact stiffness in a compliance model. Noting that the inconsistency of the Painlevé–Klein system is originated by two bilateral constraints, we cannot naturally extend his conclusion into the Painlevé paradox that is essentially due to the combined effects of friction and unilateral constraints.

The objective of this paper is to theoretically prove the existence of the tangential impact, which occurs when a rigid-body system with unilateral constraints meets the inconsistent mode of Painlevé paradox. Without loss of generality, we will adopt the Painlevé's example of a sliding rough rod to establish a varying-structure model that includes friction and compliance. Suppose that the friction satisfies Coulomb's friction law and the compliance complies with a simple model of a linear spring. Asymptotic analysis will be performed by allowing the spring stiffness to diverge to infinity. Since the frictional contact state may change from a slip to stick state, possible discontinuity of the dynamics related to the state transitions will be encompassed in our theoretical analysis.

Noting that a mathematical definition for an impact is related to a Dirac function specified to contact force, we need to obtain the theoretical expression of the contact force with respect to time, and analyze its evolution accompanying the increase of the contact stiffness. For achieving this purpose, we propose a differential comparison theorem to find the range of the solutions of the full-order model with contact compliance. By the theoretical solutions, we confirm that the Painlevé paradox truly results in a tangential impact as the contact stiffness is large enough. In addition, the rich structure in the specific impact is also exposed clearly. Accompanying the variation of friction state, the rod dynamics in the Painlevé's paradox consists of three distinct phases described as follows: *An initial period of sliding* which allows contact force to go divergence with the increase of contact stiffness, *a period of sticking* which ends at the occurrence of a reverse slip motion, and *a reverse slip phase* which causes the rod to be detached from the contact surface.

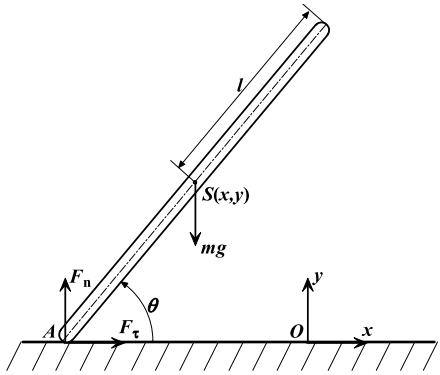

Fig. 1 A rigid rod sliding on a rough surface

The rest of the paper is organized as follows: In Sect. 2, the Painlevé's example of a sliding rough rod is reviewed with nondimensional description for its dynamics. In Sect. 3, we present preliminary knowledge needed in qualitative analysis, in which a differential comparison theorem is given, and the properties of the coefficients in differential equations are discussed. Section 4 presents the theoretical results for the time scales related to the crucial events occurring in the hybrid model. We conclude the existence of a tangential impact in Sect. 5, and end the paper in Sect. 6 with a summary and discussion.

2 Brief review for the problem of Painlevé paradox

Essentially the Painlevé's example of a sliding rough rod is a good representation of manifesting the paradox when modeling mechanical system with a single contact by a constrained-based method. In this section, we briefly review the results related to the Painlevé's example, which have been reported in a tremendous amount of literature [4, 10, 12, 13, 20, 21, 35].

2.1 Governing equations of the rod dynamics

Figure 1 depicts a rigid rod sliding on a rough surface. The rod has mass m, length $2l$ and moment of inertia $J = ml^2/3$ about its center of mass S. Let $(O - xy)$ represent an inertial frame fixed on the rough surface. By limiting it to a planar motion, the rigid rod possesses three degrees of freedom which can be described by the x and y coordinates of its center of mass and by its angular orientation θ. Suppose that the rod contacts the rough surface at point A. The interaction at the contact point provides a contact force decomposed into the F_n and F_τ components along the normal and tangential directions of the rough plane, respectively. The rod's dynamics is then governed by

$$\begin{cases} m\ddot{x}(t) = F_\tau(t), \\ m\ddot{y}(t) = F_n(t) - mg, \\ \dfrac{1}{3}ml^2\ddot{\theta}(t) = -F_n(t)l\cos\theta(t) + F_\tau(t)l\sin\theta(t). \end{cases} \tag{1}$$

Denote by (x_A, y_A) the coordinates of the contact point A in the frame $(O - xy)$. The geometric relations between the coordinates of points A and S are

$$\begin{cases} x_A(t) = x(t) - l\cos\theta(t), \\ y_A(t) = y(t) - l\sin\theta(t). \end{cases} \tag{2}$$

By differentiating (2) twice with respect to time, together with (1), the motion of the rod is equally governed by

$$\begin{cases} \ddot{y}_A = \dfrac{1+3\cos^2\theta}{m}F_n - \dfrac{3\sin\theta\cos\theta}{m}F_\tau + l\dot{\theta}^2\sin\theta - g, \\ \ddot{x}_A = -\dfrac{3\sin\theta\cos\theta}{m}F_n + \dfrac{1+3\sin^2\theta}{m}F_\tau + l\dot{\theta}^2\cos\theta, \\ \dfrac{1}{3}ml^2\ddot{\theta} = -F_n l\cos\theta + F_\tau l\sin\theta, \end{cases} \tag{3}$$

where the time variable t involved in the coordinates $x_A(t)$, $y_A(t)$ and $\theta(t)$ is omitted for simplicity.

In order to make (3) solvable, there are two methods to determine the normal contact force F_n: (i) a constraint-based method that models a sustained contact as a constraint equation in association with the geometries of contacting bodies [20, 21, 35], and (ii) a compliance-based method [12, 13] that takes a constitutive relationship to scale the material behavior at the lumped contact point.

In the constraint-based method, the distance function $y_A = 0$ is thought of as a constraint applied in the rod system. In this case, the normal acceleration $\ddot{y}_A$ and the normal force F_n form a complementary pair [23] as they must satisfy

$$\ddot{y}_A \geq 0, \quad F_n \geq 0, \quad F_n \cdot \ddot{y}_A = 0. \tag{4}$$

Note that Eq. (4) is a consequence of the complementary conditions $0 \leq y_A(t) \perp F_n(t) \geq 0$, so we have to add this to the model (3).

When a compliant-based model is used, a constitutive relationship between the normal deformation and the normal contact force at point A is needed. If the material adjacent to the contact behaves in elasticity without any dissipation of energy, we can prescribe a linear spring with a lumped stiffness parameter K to approximately represent the interaction between the rod and the rough surface. Denote by δ the normal deformation in the contact compliance, and suppose that the constraint equation $y_A = 0$ is satisfied exactly only when there is contact with zero normal force. In this case, we can write F_n as

$$F_n = \begin{cases} K\delta, & \text{if } \delta \geq 0, \\ 0, & \text{if } \delta < 0. \end{cases} \tag{5}$$

Assuming that the deformation only occurs at the contact interface, we have $\delta = -y_A$ and also $\dot{\delta} = -\dot{y}_A$, $\ddot{\delta} = -\ddot{y}_A$. This makes the first equation in (3) directly become a second ordinary differential equation for the variable δ whose evolution governs the change of normal contact force F_n.

Coulomb's friction law states a relationship between F_n and F_τ as:

$$\begin{cases} F_\tau = -\mu F_n \operatorname{sign}(\dot{x}_A), & \text{if } \dot{x}_A \neq 0;\ \text{sliding state}, \\ |F_\tau| \leq \mu_s F_n, & \text{if } \dot{x}_A = 0;\ \text{sticking state}, \end{cases} \tag{6}$$

where $\text{sign}(\dot{x}_A) = 1$ as $\dot{x}_A > 0$ and $\text{sign}(\dot{x}_A) = -1$ when $\dot{x}_A < 0$. μ and μ_s represent the sliding and static coefficients of friction, respectively. Usually, the value of μ_s is much larger than the one of μ [38].

In most cases, both the constraint- and compliance-based methods can effectively solve the forward dynamics equations. Due to the peculiarity of Coulomb's friction, however, inconsistent or multiple solutions may appear in the constraint-based method, corresponding to the problem of the Painlevé paradox.

2.2 Painlevé paradox

Before discussing the problem of the Painlevé paradox, we follow Mamaev [21] to choose $\sqrt{l/g}$ to be the unit of time and l the unit of distance. Namely, we make a change of coordinates and time in the equations by

$$\frac{x_A}{l} \longmapsto x_A, \qquad \frac{y_A}{l} \longmapsto y_A, \qquad \sqrt{\frac{g}{l}}t \longmapsto t. \tag{7}$$

Moreover, we define the following dimensionless quantities:

$$\frac{F_n}{mg} \longmapsto F_n, \qquad \frac{F_\tau}{mg} \longmapsto F_\tau. \tag{8}$$

Here we adopt the same symbols to represent the dimensionless quantities for simplicity. After doing that, Eq. (3) is rewritten as

$$\begin{cases} \ddot{y}_A = (1 + 3\cos^2\theta)F_n - (3\sin\theta\cos\theta)F_\tau + \dot{\theta}^2\sin\theta - 1, \\ \ddot{x}_A = -(3\sin\theta\cos\theta)F_n + (1 + 3\sin^2\theta)F_\tau + \dot{\theta}^2\cos\theta, \\ \dfrac{1}{3}\ddot{\theta} = -F_n\cos\theta + F_\tau\sin\theta. \end{cases} \tag{9}$$

Suppose that the rod slides leftwards with tangential velocity $\dot{x}_A < 0$. Thus, the friction at contact point A states that $F_\tau = \mu F_n$. In this case, Eq. (3) become:

$$\begin{cases} \ddot{y}_A = A(\theta,\mu)F_n + B(\theta,\dot{\theta}), \\ \ddot{x}_A = C(\theta,\mu)F_n + D(\theta,\dot{\theta}), \\ \ddot{\theta} = P(\theta,\mu)F_n, \end{cases} \tag{10}$$

where

$$\begin{aligned} &A(\theta,\mu) = \big(1 + 3\cos\theta(\cos\theta - \mu\sin\theta)\big), \qquad B(\theta,\dot{\theta}) = \dot{\theta}^2\sin\theta - 1, \\ &C(\theta,\mu) = \big(\mu + 3\sin\theta(-\cos\theta + \mu\sin\theta)\big), \qquad D(\theta,\dot{\theta}) = \dot{\theta}^2\cos\theta, \\ &P(\theta,\mu) = 3(-\cos\theta + \mu\sin\theta). \end{aligned} \tag{11}$$

As the constraint-based method is used, solution existence and uniqueness can be easily distinguished according to the complementarity pair (4) together with the first equation in (10). If and only if $A(\theta,\mu) > 0$, the solution obtained from the constraint-based method is unique for all $B(\theta,\dot{\theta})$ [18, 28]. If $A(\theta,\mu) < 0$, the normal contact force F_n is either in an inconsistent mode if $B(\theta,\dot{\theta}) < 0$, or is in an indeterminate mode if $B(\theta,\dot{\theta}) > 0$.

As normal deformation is considered in modeling, the resulting dynamical equation is given by

$$\begin{cases} \ddot{\delta} = -\dfrac{1}{\kappa} A(\theta, \mu)\delta - B(\theta, \dot{\theta}), \\ \ddot{x}_A = \dfrac{1}{\kappa} C(\theta, \mu)\delta + D(\theta, \dot{\theta}), \\ \ddot{\theta} = \dfrac{1}{\kappa} P(\theta, \mu)\delta, \end{cases} \tag{12}$$

where

$$\frac{\delta}{l} \longmapsto \delta, \qquad \frac{K}{mg/l} \longmapsto \frac{1}{\kappa} \tag{13}$$

are dimensionless quantities complying with the definition in the constraint-based model. As $K \to \infty$, the small parameter κ goes to zero to recover the limit of a rigid body model.

Noting that δ varies faster than variables x_A and θ, we denote δ as the fast variable while x_A and θ are the slow variables [8]. Comparing with the constraint-based model, Eq. (12) contains a small oscillation confined to a boundary layer that is related to the fast variable δ. Basically, we can evaluate the equilibrium solution $\bar{\delta}$ of the small oscillation by setting $\kappa\ddot{\delta} = 0$. If $\bar{\delta}$ is positive and exponentially stable, the slow dynamics represented by the last two equations of (12) can be approximately solved through substitution of $\bar{\delta}$. Therefore, the precondition of using a constraint-based model is that the boundary layer dynamics is exponentially stable [8, 10].

Corresponding to the Painlevé paradox where $A(\theta, \mu) < 0$, it is clear that the boundary layer is unstable. The objective of this paper is to prove that the instability occurring in the inconsistent mode ($B(\theta, \dot{\theta}) < 0$ and $A(\theta, \mu) < 0$) truly manifests an impulsive process at the limit $\kappa \to 0$.

3 Preliminary knowledge for qualitative analysis

In this section, we present preliminary knowledge needed in the qualitative analysis of the Painlevé paradox.

3.1 Two lemmas in differential inequalities

By Zygmund's classical theorem on monotone functions [39], we know that a continuous function $x(t)$ in a time interval $\mathcal{T} = [t_0, +\infty)$ increases monotonically if its derivative $\dot{x}(t)$ is always positive. From this theorem, we easily analyze the global property of linear second order differential equations with time-varying coefficients.

Lemma 1 *Let $a(t) \in C^2([t_0, \infty), \mathbb{R})$ and $b(t) \in C^2([t_0, \infty), \mathbb{R})$ on a time interval $\mathcal{T} = [t_0, +\infty)$. Suppose that $x(t)$ and $\dot{x}(t)$ are the solutions of the linear differential equation*:

$$\ddot{x}(t) = a(t)x(t) + b(t), \tag{14}$$

starting from an initial state: $x(t_0) \geq 0, \dot{x}(t_0) \geq 0$. *If $a(t) > 0$ and $b(t) > 0$ are always satisfied on $\mathcal{T}$, then both $x(t)$ and $\dot{x}(t)$ increase monotonically, and $x(t) > x(t_0)$, $\dot{x}(t) > \dot{x}(t_0)$ for all $t \in \mathcal{T}$.*

Proof For each $x(t_0)$ and $\dot{x}(t_0)$, Eq. (14) has, from conventional arguments, a unique solution of class C^2 on $t \in [t_0, +\infty)$. By setting $z_1 \triangleq x$ and $z_2 \triangleq \dot{x}$, we have $\dot{z}_2(t) = a(t)z_1(t) + b(t)$. As $z_1(t_0) \geq 0$, $a(t) > 0$, and $b(t) > 0$, we get $\dot{z}_2(t_0) > 0$. By continuity necessarily there exists $\epsilon > 0$ such that $\dot{z}_2(t) > 0$. Consequently, both $z_1(t)$ and $z_2(t)$ on $[t_0, t_0 + \epsilon]$ increase monotonically. By concatenation and since solutions exist uniquely, the conclusion follows. □

In terms of Lemma 1, we can compare the solution in (14) with the one of a linear ODE system with constant coefficients ω and η:

$$\ddot{y}(t) = \omega^2 y(t) + \eta. \tag{15}$$

Lemma 2 *Suppose that the coefficients in* (14) *and* (15) *satisfy* $a(t) > \omega^2$ *and* $b(t) > \eta > 0$ *on a time interval* $\mathcal{T} \in [t_0, \infty)$. *When the two systems start from the same initial conditions, i.e.,* $x(t_0) = y(t_0) \geq 0$, *and* $\dot{x}(t_0) = \dot{y}(t_0) \geq 0$, *we have* $x(t) \geq y(t) \geq 0$, $\dot{x}(t) \geq \dot{y}(t) \geq 0$ *for all* $t \in \mathcal{T}$.

Proof By setting $\xi \triangleq x - y$, $\xi_1 = \xi$, $\xi_2 = \dot{\xi}$, from (14) and (15) we get an *error dynamics* expressed as follows:

$$\begin{cases} \dot{\xi}_1 = \xi_2, \\ \dot{\xi}_2 = a(t)\xi_1 + \beta(t), \\ \xi_1(0) = 0, \qquad \xi_2(0) = 0, \end{cases} \tag{16}$$

with $\beta(t) = b(t) - \eta + (a(t) - \omega^2)y(t) > 0$.

Clearly, (16) satisfies the conditions in Lemma 1. For the same reason as in Lemma 1, the proof follows. □

We remark that system (15), whose analytical solution can be easily obtained, corresponds to a lower boundary system for the specific system (14). Similarly, an upper boundary system with an analytical solution can also be defined for (14). Some applications of the two lemmas will be given below.

3.2 Properties of the coefficients in paradox

The configuration of the sliding rough rod is limited in a range $\theta \in (0, \pi)$. For a given μ, all the coefficients $A(\theta, \mu)$, $C(\theta, \mu)$ and $P(\theta, \mu)$ are single-valued and even analytic functions with respect to θ. As $\theta \in (0, \pi)$, through a simple calculation, the value of $A(\theta, \mu)$ is found to be limited in a range as follows:

$$\frac{1}{2}\left(5 - 3\sqrt{1+\mu^2}\right) \leq A(\theta, \mu) \leq \frac{1}{2}\left(5 + 3\sqrt{1+\mu^2}\right). \tag{17}$$

Clearly, the value of $A(\theta, \mu)$ can become negative if and only if $\mu > 4/3$. When the value of μ is superior to the threshold, the value of θ which gives $A(\theta, \mu) < 0$ is not null, and is confined in a region given by [18, 28]

$$\frac{3\mu - \sqrt{9\mu^2 - 16}}{2} \leq \tan\theta \leq \frac{3\mu + \sqrt{9\mu^2 - 16}}{2}. \tag{18}$$

By (18) and $\mu > 4/3$, we easily know that Painlevé paradox can occur only if the leftward-sliding rod is in a configuration $0 < \theta < \pi/2$. In the following, we always assume $\mu > 4/3$, thus $\cos\theta > 0$ and $\sin\theta > 0$.

To initialize the rod in an inconsistent mode at time t_0, we select an initial configuration $\theta(t_0)$ satisfying (18), and specify $\dot{\theta}(t_0)$ with a value permitting $B(\theta(t_0), \dot{\theta}(t_0)) < 0$. By (11), this limits the absolute value of the initial angular velocity in a range $|\dot{\theta}(t_0)| < \sqrt{1/\sin\theta(t_0)}$.

For simplicity, we denote $A(\theta(t), \mu)$ as $A(t)$, $B(\theta(t), \dot{\theta}(t))$ as $B(t)$, and so on. By continuity of the state trajectories, there exists a time interval $\mathcal{T}_0 = [0, \varepsilon_0]$, $\varepsilon_0 > 0$, satisfying the condition $A(t) < 0$ and $B(t) < 0$. This allows us to specify two domains $\mathcal{D}(A)$ and $\mathcal{D}(B)$ for $A(t)$ and $B(t)$, respectively.

$$\begin{cases} \mathcal{D}(A) = \{-M_2 \le A(t) \le -M_1 < 0\}, & M_1 < -A(t_0),\ M_2 > -(5 - 3\sqrt{1+\mu^2})/2, \\ \mathcal{D}(B) = \{-\eta_2 \le B(t) \le -\eta_1 < 0\}, & \eta_1 < -B(t_0),\ \eta_2 > 1. \end{cases} \tag{19}$$

Here the values of M_i and η_i $(i = 1, 2)$ are positive. In the above definition, the left bound of $\mathcal{D}(A)$ takes a value $(-M_2)$ less than the minimum of $A(t)$ (see Eq. (17)), while its right bound takes a value $(-M_1)$ greater than its initial value. Noting that $\dot{\theta}(t) = 0$ makes $B(t)$ take a minimum value $B(t) = -1$, similar definition is also assigned to $\mathcal{D}(B)$. As $\mathcal{D}(A)$ and $\mathcal{D}(B)$ are defined by (19), only their right bounds can be accessible on $\mathcal{T}_0$.

Now let us analyze the properties of coefficients $C(t)$ and $P(t)$ as $A(t) < 0$ and $B(t) < 0$. Note that $C(t)$, as $A(t)$, is an analytic function of θ. Using its expression, together with $A(t) \in \mathcal{D}(A)$, we have

$$\mu + (M_1 + 1)\tan\theta \le C(t) \le \mu + (M_2 + 1)\tan\theta. \tag{20}$$

By (18) for the range of value of $\tan\theta$, it follows that $C(t)$ is always positive and bounded. Similarly, from the expression of $P(t)$, we get

$$\frac{1}{\cos\theta} \le P(t) = 3(-\cos\theta + \mu\sin\theta) \le 3\sqrt{1+\mu^2}. \tag{21}$$

Since $A(t) \in \mathcal{D}(A)$, it is clear that $P(t)$ is also positive and bounded when θ is limited in the range defined by Eq. (18). According to the expression $D(t) = \dot{\theta}^2\cos\theta$, together with the condition $B(t) \in \mathcal{D}(B)$, we get

$$D(t) = \dot{\theta}^2\cos\theta = \frac{1 + B(t)}{\tan\theta}, \tag{22}$$

which means that $D(t)$ is positive and bounded when θ is limited in the range defined by (18).

4 Possible events and time scales analysis

In this section, we will analyze the dynamical equations (12) when their coefficients are limited in the ranges $A(t) \in \mathcal{D}(A)$ and $B(t) \in \mathcal{D}(B)$. It is worth noting that, accompanying the evolution of $A(t)$ and $B(t)$, the tangential velocity of the moving contact point may vanish. At that instant, a stick–slip transition occurs, such that the relationship between F_n and F_τ changes. Therefore, Eq. (12) will be invalid for the subsequent motion of the rod. In order to understand what happens as $\kappa \to 0$, the time scale related to the occurrence of the crucial event should be discussed.

4.1 Possible events

Let us recall the governing equations given by (12), in which fast and slow dynamics equations are strongly coupled together through the time-varying coefficients $A(t)$, $B(t)$, $C(t)$, $D(t)$, and $P(t)$. Note that the values of $A(t)$ and $B(t)$ vary at different rates with respect to time, and only their right bounds in $\mathcal{D}(A)$ and $\mathcal{D}(B)$ are accessible. Let us denote by ε_A and ε_B the instants when $A(t)$ and $B(t)$ attain the right bounds of $\mathcal{D}(A)$ and $\mathcal{D}(B)$, respectively.

Since $A(t) \in \mathcal{D}(A)$ and $B(t) \in \mathcal{D}(B)$ are satisfied, we know that both $C(t)$ and $D(t)$ are positive and bounded. Note that the horizontal dynamics given by the second equation in (12) is initialized by $\dot{x}_A(t_0) < 0$. When $C(t)$ and $D(t)$ are positive and bounded, the magnitude of $|\dot{x}_A(t)|$ will decrease monotonically. This means that $|\dot{x}_A(t)|$ may vanish at a certain instant $\varepsilon_{\dot{x}_A}$, though the conditions $A(t) \in \mathcal{D}(A)$ and $B(t) \in \mathcal{D}(B)$ defined on a time interval $\mathcal{T}_0$ are still satisfied. In summary, there are three possible events: either the right bound of $\mathcal{D}(A)$ or the one of $\mathcal{D}(B)$ is attained at ε_A or ε_B, respectively, or $\dot{x}_A(t = \varepsilon_{\dot{x}_A}) = 0$, which may occur in the rod dynamics.

To distinguish the three possible events, we should separately compute the values of $\varepsilon_{\dot{x}_A}$, ε_A and ε_B, then compare them to determine which one of the three events occurs first. As time goes on from the initial time t_0, we can designate a time interval $\mathcal{T}_1 = [t_0, t_1]$, and suppose that at the end of $\mathcal{T}_1$ there is one event of either $\dot{x}_A(t_1) = 0$, or $A(t_1) = -M_1$, or $B(t_1) = -\eta_1$ which occurs. The definition for $\mathcal{T}_1$ allows us to conveniently perform time scale analysis by separately computing the values of $\varepsilon_{\dot{x}_A}$, ε_A and ε_B.

4.2 Time scale analysis

Let us specify $t_0 = 0$ and the initial state of the dynamical model in (12) as follows: $\delta(0) = \dot{\delta}(0) = 0, \theta(0) = \theta^0, \dot{\theta}(0) = \dot{\theta}^0, \dot{x}_A(0) = \dot{x}_A^0 < 0$. It is worth noting that θ^0 and $\dot{\theta}^0$ take values that allow $A(0) < 0$ and $B(0) < 0$ under the coefficient of friction μ. Based on the initial values of $A(0)$ and $B(0)$, we follow the definition in (19) to define the domains $\mathcal{D}(A)$ and $\mathcal{D}(B)$.

For the given domains $\mathcal{D}(A)$ and $\mathcal{D}(B)$ and initial states, the values of $\varepsilon_{\dot{x}_A}$, ε_A and ε_B are just influenced by the stiffness coefficient κ. In the following, we expect to obtain the values of $\varepsilon_{\dot{x}_A}$, ε_A and ε_B with respect to the parameter κ. Once this is done, we can obtain knowledge about the time scales experienced by the three possible events, then determine which event occurs first at the end of $\mathcal{T}_1$.

To obtain the values of $\varepsilon_{\dot{x}_A}$, ε_A and ε_B with respect to κ, we need to perform calculation for the small normal deformation $\delta(t)$ in the boundary layer around the contact point. Noting that the coefficients $A(t)$ and $B(t)$ are time-varying and coupled with the states of the slow dynamics in the rod motion, let us estimate the value of $\delta(t)$ by constructing two linear oscillating systems defined as follows:

$$\begin{cases} \ddot{\delta}_l(t) = \dfrac{M_1}{\kappa}\delta_l(t) + \eta_1, \\ \ddot{\delta}_r(t) = \dfrac{M_2}{\kappa}\delta_r(t) + \eta_2, \end{cases} \tag{23}$$

which are obtained from the first equation in (12), replacing $A(t)$ and $B(t)$ by their upper and lower bounds in (19).

By specifying the initial state of the dynamical model in (12) to the two linear oscillating systems (23), their analytical solutions are given by

$$\begin{cases} \delta_l(t) = \dfrac{\eta_1}{2\omega_l^2} e^{\omega_l t} + \dfrac{\eta_1}{2\omega_l^2} e^{-\omega_l t} - \dfrac{\eta_1}{\omega_l^2} > 0, \\ \delta_r(t) = \dfrac{\eta_2}{2\omega_r^2} e^{\omega_r t} + \dfrac{\eta_2}{2\omega_r^2} e^{-\omega_r t} - \dfrac{\eta_2}{\omega_r^2} > 0, \end{cases} \tag{24}$$

where $\omega_l^2 = M_1/\kappa$, $\omega_r^2 = M_2/\kappa$.

According to Lemma 2, Eq. (24) gives the lower and upper bounds for the normal deformation $\delta(t)$ on $\mathcal{T}_1$. Therefore, as $A(t) \in \mathcal{D}(A)$ and $B(t) \in \mathcal{D}(B)$, we easily deduce the following properties that are satisfied by the rod state on $\mathcal{T}_1$:

1. The absolute value of $\dot{x}_A(t)$ decreases monotonically because $\dot{x}_A^0 < 0$ while $\ddot{x}_A(t) = \frac{1}{\kappa}C(t) + D(t) > 0$.
2. The angular velocity $\dot{\theta}(t)$ increases monotonically and is bounded for similar reasons.
3. The normal deformation and its rate are confined in the ranges $0 \le \delta_l(t) \le \delta(t) \le \delta_r(t)$, $0 \le \dot{\delta}_l(t) \le \dot{\delta}(t) \le \dot{\delta}_r(t)$.

Now let us compute the value of ε_A. In this case, $A(t)$ varies from $A(t_0)$ to $-M_1$ while $B(t) \in \mathcal{D}(B)$ and $\dot{x}_A(t) < 0$ for all $t \in \mathcal{T}_1$. Since $A(t)$ is a bounded analytic function with respect to $\theta(t)$, the variation of the angle, $\Delta\theta$, is a finite value as time goes from t_0 to t_1. Note that $\dot{\theta}(t)$ increases monotonically and is bounded ($B(t) \in \mathcal{D}(B)$). The positive and bounded values of $\theta(t)$ and $\dot{\theta}(t)$ mean that the value of ε_A can be approximately estimated by $\varepsilon_A > \Delta\theta/\bar{\dot{\theta}}_{\max}$, where $\bar{\dot{\theta}}_{\max}$ is the maximum of angular velocity when $B(t) \in \mathcal{D}(B)$. Therefore, one has

$$\varepsilon_A = \mathcal{O}\big(\kappa^0\big), \tag{25}$$

which means that the value of ε_A, as both $\mathcal{D}(A)$ and $\mathcal{D}(B)$ have been specified previously, is barely influenced by the contact stiffness parameter. This point is easily understood because $\theta(t)$ is essentially a slow variable with respect to time.

In order to compute the value of $\varepsilon_{\dot{x}_A}$, we suppose that $\dot{x}_A(\varepsilon_{\dot{x}_A}) = 0$, while $A(t) \in \mathcal{D}(A)$ and $B(t) \in \mathcal{D}(B)$ for all $t \in \mathcal{T}_1 = [0, \varepsilon_{\dot{x}_A}]$. In this case, integration of the horizontal dynamics of (12) over $\mathcal{T}_1$ leads to

$$-\dot{x}_A^0 = \int_0^{\varepsilon_{\dot{x}_A}} \left(\frac{1}{\kappa} C(t)\delta(t) + D(t) \right) dt. \tag{26}$$

On $\mathcal{T}_1$, we have $0 \le \delta_l(t) \le \delta(t) \le \delta_r(t)$, $C(t) > 0$, and $D(t) > 0$. Moreover, both $C(t)$ and $D(t)$ are bounded such that (26) can satisfy an inequality expressed as follows:

$$-\dot{x}_A^0 \ge \int_0^{\varepsilon_{\dot{x}_A}} \frac{1}{\kappa} \underline{C}\delta(t)\, dt, \tag{27}$$

where $\underline{C}$ is the lower border of $C(t)$ on $\mathcal{T}_1$. Substituting the solution $\delta_l(t)$ in (24) into the inequality, we have

$$-\dot{x}_A^0 > \frac{\underline{C}\eta_1}{2M_1\omega_l} e^{\omega_l \varepsilon_{\dot{x}_A}} - \frac{\underline{C}\eta_1}{2M_1\omega_l} e^{-\omega_l \varepsilon_{\dot{x}_A}} - \frac{\underline{C}\eta_1}{M_1} \varepsilon_{\dot{x}_A}. \tag{28}$$

Note that ω_l increases as κ decreases. For a given value of $\dot{x}_A^0 < 0$, there exists a small value of κ_1, such that for all $\kappa < \kappa_1$, the term $e^{\omega_l \varepsilon_{\dot{x}_A}}$ can be expanded by Taylor series:

$$e^{\omega_l \varepsilon_{\dot{x}_A}} \approx 1 + \omega_l \varepsilon_{\dot{x}_A} + \frac{1}{2}\omega_l^2 \varepsilon_{\dot{x}_A}^2 + \mathcal{O}\big(\varepsilon_{\dot{x}_A}^3\big). \tag{29}$$

Then, inequality (28) is rewritten as (neglecting cubic terms):

$$\left(\varepsilon_{\dot{x}_A} - \frac{1}{\omega_l}\right)^2 < -\dot{x}_A(0)\frac{4M_1}{\underline{C}\eta_1\omega_l} + \frac{2}{\omega_l^2}e^{-\omega_l \varepsilon_{\dot{x}_A}} - \frac{1}{\omega_l^2}, \quad \forall \kappa < \kappa_1. \tag{30}$$

By considering $0 < e^{-\omega_l \varepsilon_{\dot{x}_A}} < 1$, we estimate an upper bound of $\varepsilon_{\dot{x}_A}$ as follows:

$$\varepsilon_{\dot{x}_A} < \frac{1}{\omega_l} + \sqrt{-\frac{4M_1}{\underline{C}\eta_1\omega_l}\dot{x}_A^0 + \frac{1}{\omega_l^2}} \sim \mathcal{O}\big(\sqrt[4]{\kappa}\big), \quad \forall \kappa < \kappa_1. \tag{31}$$

Similarly, we can also estimate a lower bound of $\varepsilon_{\dot{x}_A}$. Denote by $\overline{C}$ and $\overline{D}$ the upper bounds of $C(t)$ and $D(t)$ on $\mathcal{T}_1$, respectively. By (26), together with the substitution of $\delta_r(t)$ for $\delta(t)$, we get

$$-\dot{x}_A^0 < \frac{\overline{C}\eta_2}{2M_2\omega_r}e^{\omega_r \varepsilon_{\dot{x}_A}} - \frac{\overline{C}\eta_2}{2M_2\omega_r}e^{-\omega_r \varepsilon_{\dot{x}_A}} + \left(\overline{D} - \frac{\overline{C}\eta_2}{M_2}\right)\varepsilon_{\dot{x}_A}. \tag{32}$$

Note that the second term on the right-hand side of (32) is negative. Moreover, $(\overline{D} - \frac{\overline{C}\eta_2}{M_2})$ takes a finite value. Thus, the last two terms on the right-hand side of (32) can be ignorable in the qualitative analysis. So we estimate the lower bound of $\varepsilon_{\dot{x}_A}$ as follows:

$$\varepsilon_{\dot{x}_A} > \frac{1}{\omega_r}\left[\ln\left(\omega_r \frac{-2M_2\dot{x}_A^0}{\overline{C}\eta_2}\right)\right] \sim \mathcal{O}\left(\sqrt{\kappa}\ln\left(\frac{1}{\sqrt{\kappa}}\right)\right). \tag{33}$$

By (31) and (33), and only concerning the terms related to the order of parameter κ, we can confirm that, as $\kappa < \kappa_1$, the value of $\varepsilon_{\dot{x}_A}$ is limited in a range

$$\mathcal{O}\left(\sqrt{\kappa}\ln\left(\frac{1}{\sqrt{\kappa}}\right)\right) < \varepsilon_{\dot{x}_A} < \mathcal{O}\big(\sqrt[4]{\kappa}\big), \quad \forall \kappa < \kappa_1. \tag{34}$$

We now compute the value of ε_B by assuming that $B(\varepsilon_B) = -\eta_1$ while $A(t) \in \mathcal{D}(A)$, and $\dot{x}_A(t) < 0$ for all $t \in \mathcal{T}_1 = [0, \varepsilon_B]$. In this case, we need to investigate the attitude dynamics in the rod motion.

Integrating the third equation in (12) on $\mathcal{T}_1$, we get

$$\Delta\dot{\theta} = \int_0^{\varepsilon_B} \frac{1}{\kappa}P(t)\delta(t)\,dt. \tag{35}$$

Note that $\dot{\theta}(t)$ increases monotonically and is bounded as $B(t) \in \mathcal{D}(B)$, such that $\Delta\dot{\theta} > 0$ and it is bounded with a finite value. Moreover, we know that $P(t)$ and $\delta(t)$ are positive and bounded on $\mathcal{T}_1$. Substituting $\delta(t)$ in (35) by the solution $\delta_r(t)$ in (24), we get the following inequality:

$$\Delta\dot{\theta} < \overline{P}\frac{\eta_2}{M_2}\left(\frac{1}{2\omega_r}e^{\omega_r\varepsilon_B} - \frac{1}{2\omega_r}e^{-\omega_r\varepsilon_B} - \varepsilon_B\right) < \frac{\overline{P}\eta_2}{2M_2\omega_r}e^{\omega_r\varepsilon_B}, \tag{36}$$

where $\overline{P}$ is the upper bound of $P(t)$ on $\mathcal{T}_1$.

So a lower bound for ε_B is given by

$$\varepsilon_B > \frac{1}{\omega_r}\ln\left(\frac{2M_2\Delta\dot{\theta}}{\overline{P}\eta_2}\omega_r\right) \sim \mathcal{O}\left(\sqrt{\kappa}\ln\left(\frac{1}{\sqrt{\kappa}}\right)\right). \tag{37}$$

Similarly, substituting $\delta(t)$ in (35) by the solution $\delta_l(t)$ in (24), together with the lower bound $\underline{P}$ for $P(t)$ on $\mathcal{T}_1$, we obtain

$$\Delta\dot{\theta} > \underline{P}\frac{\eta_1}{M_1}\left(\frac{1}{2\omega_l}e^{\omega_l\varepsilon_B} - \frac{1}{2\omega_l}e^{-\omega_l\varepsilon_B} - \varepsilon_B\right). \tag{38}$$

Note that the value of $\Delta\dot{\theta}$ is positive and bounded on $\mathcal{T}_1$. So there exists a small value of κ_2, such that for all $\kappa < \kappa_2$, we can use Taylor series to expand the term $e^{\omega_l\varepsilon_B}$. Then, we estimate the upper bound for ε_B with a value given by

$$\varepsilon_B < \sqrt{\frac{4M_1\Delta\dot{\theta}}{\underline{P}\eta_1\omega_l} + \frac{1}{\omega_l^2}} + \frac{1}{\omega_l}, \quad \forall\kappa < \kappa_2. \tag{39}$$

By (37) and (39), we know that the value of ε_B is confined in a range expressed as follows:

$$\mathcal{O}\left(\sqrt{\kappa}\ln\left(\frac{1}{\sqrt{\kappa}}\right)\right) < \varepsilon_B < \mathcal{O}\left(\sqrt[4]{\kappa}\right), \quad \forall\kappa < \kappa_2. \tag{40}$$

In terms of the values of ε_A, $\varepsilon_{\dot{x}_A}$ and ε_B given respectively by (25), (34) and (40), we conclude as follows:

As an initial state is specified to the rod dynamics and domains $\mathcal{D}(A)$ and $\mathcal{D}(B)$ are given in advance, we can always find a suitable $\kappa^* = \min(\kappa_1, \kappa_2)$, such that for all $\kappa < \kappa^*$, $A(t)$ can still remain in the domain $\mathcal{D}(A)$.

The analysis shown above indicates that $\varepsilon_{\dot{x}_A}$ and ε_B take the same order with respect to κ. This means that the occurrence of $\dot{x}_A(t) = 0$ is not necessary for a given domain $\mathcal{D}(B)$. Note that the event $\dot{x}_A(t) = 0$ may change the friction status from a slip to a stick state, then stabilize the boundary layer dynamics. For confirming that the occurrence of the event $\dot{x}_A(t) = 0$ is unavoidable in the rod dynamics, we need to investigate the rod motion when $\mathcal{T}_1$ ends at the instant ε_B instead of $\varepsilon_{\dot{x}_A}$.

4.3 An unavoidable event related to tangential velocity vanishing

At the instant $t_1 = \varepsilon_B$, the motion of the rod takes a state as follows: $B(\varepsilon_B) = -\eta_1$, $\dot{x}_A(\varepsilon_B) < 0$, $\delta(\varepsilon_B) \geq \delta_l(\epsilon_B) > 0$, $\dot{\delta}(\varepsilon_B) \geq \dot{\delta}_l(\epsilon_B) > 0$, and $-M_2 < A(\varepsilon_B) < -M_1$. After $t_1 = \varepsilon_B$, Eq. (12) is still valid to govern the rod dynamics until the event $\dot{x}_A(t) = 0$ occurs.

Let us suppose that the tangential velocity can vanish at time ε_2, namely $\dot{x}_A(\varepsilon_2) = 0$, and $\varepsilon_2 > \varepsilon_B$. By (25) we know $\varepsilon_A = \mathcal{O}(\xi^0)$ under the condition of $\dot{\theta}(t)$ bounded and $A(t) \in \mathcal{D}(A)$. To obtain the value of ε_2 and qualitatively analyze the rod motion after $t_1 = \varepsilon_B$, we first introduce an assumption as follows:

Assumption On the time interval $\mathcal{T}_2 = [\varepsilon_B, \varepsilon_2]$, the value of $A(t)$ remains in the domain $\mathcal{D}(A)$ prescribed previously.

This assumption is reasonable if the obtaining value of ε_2 takes an order of κ greater than zero, and $\dot{\theta}(t)$ is bounded on $\mathcal{T}_2$. In the following, we will prove that the precondition responsible for the assumption is true.

Under the condition $A(t) \in \mathcal{D}(A)$, we know that $C(t)$ and $P(t)$ are positive and bounded since both of them are single-valued and analytic functions with respect to $\theta(t)$. By integrating the second equation in (12) over the time interval $[0, \varepsilon_2]$, together with $\dot{x}_A(\varepsilon_2) = 0$, we get

$$-\dot{x}_A^0 = \int_0^{\varepsilon_2} \frac{1}{\kappa}\big(C(t)\delta(t) + D(t)\big)\, dt. \tag{41}$$

Denote $I(\varepsilon_2) = \int_0^{\varepsilon_2} \delta(t)\, dt$ and by $\underline{C}$ the lower bound of $C(t)$. By noting that $D(t)$ in (11) is always positive, we have

$$\int_0^{\varepsilon_2} \delta(t)\, dt \triangleq I(\varepsilon_2) < -\frac{\kappa \dot{x}_A^0}{\underline{C}}, \tag{42}$$

in the admissible range of θ, where one notices that $-\frac{\kappa \dot{x}_A(0)}{\underline{C}} > 0$ since $\dot{x}_A(0) < 0$ and $\underline{C} > 0$. Similarly, denote by $\overline{P}$ the upper bound of $P(t)$. Integration of the third equation in (12) over $[0, \varepsilon_2]$ leads to

$$\Delta\dot{\theta} = \dot{\theta}(\varepsilon_2) - \dot{\theta}(0) = \int_0^{\varepsilon_2} \frac{1}{\kappa} P(t)\delta(t)\, dt \le \frac{1}{\kappa}\overline{P} I(\varepsilon_2) < -\frac{\overline{P}}{\underline{C}}\dot{x}_A^0. \tag{43}$$

From (43), it is clear that, if $A(t) \in \mathcal{D}(A)$, $\Delta\dot{\theta}$ is bounded on the time interval $[0, \varepsilon_2]$, such that $B(t) = \dot{\theta}^2 \sin\theta - 1$ on the same time interval is also bounded. Note that the bounded value of $B(t)$ during the time interval $[0, \varepsilon_2]$ calls for the assumption of $A(t) \in \mathcal{D}(A)$, whose existence in turn requires the condition that the value of ε_2 can be arbitrary small as κ goes to zero.

Now, let us compute the value of ε_2 by recalling the first equation in (12), which is governed by

$$\ddot{\delta}(t) = -\frac{1}{\kappa} A(t)\delta(t) - B(t), \quad t \in [0, \varepsilon_2]. \tag{44}$$

Clearly, there exists a value κ_3, such that for all $\kappa < \kappa_3$, $\ddot{\delta}(t) \ge 0$ is satisfied on the time interval $t \in [0, \varepsilon_2]$. This means that, before the crucial event $\dot{x}_A(t) = 0$ occurs, $\delta(t)$ can monotonically increase for all $\kappa < \kappa_3$. Namely, we have $\delta(t) \ge \delta(\varepsilon_B)$ when $\varepsilon_B \le t \le \varepsilon_2$.

At time $t = \varepsilon_B$, we have shown that $\delta(\varepsilon_B) > \delta_l(\varepsilon_B)$, where $\delta_l(t)$ is given by (24). From (24), together with $\kappa < \kappa_3$ and $\varepsilon_B \le t \le \varepsilon_2$, we have

$$\delta(t) \ge \delta_l(\varepsilon_B) = \frac{\eta_1}{2\omega_l^2} e^{\omega_l \varepsilon_B} + \frac{\eta_1}{2\omega_l^2} e^{-\omega_l \varepsilon_B} - \frac{\eta_1}{\omega_l^2}, \quad t \in [\varepsilon_B, \varepsilon_2]. \tag{45}$$

By (37) for the lower bound of ε_B, and using $\omega_l^2 = M_1/\kappa$, $\omega_r^2 = M_2/\kappa$ with $0 < M_1 < M_2$, the above inequality can be rewritten as

$$\delta(t) \ge \delta_l(\varepsilon_B) > \frac{\eta_1}{\omega_l^2}\left(\frac{1}{2}\left(\frac{2M_2\omega_r}{\overline{P}\eta_2}\Delta\dot{\theta}\right)^{\sqrt{M_1/M_2}} - 1\right), \quad t \in [\varepsilon_B, \varepsilon_2]. \tag{46}$$

On the time interval $t \in [\varepsilon_B, \varepsilon_2]$, the integration of the second equation in (12) leads to

$$-\dot{x}_A(\varepsilon_B) = \int_{\varepsilon_B}^{\varepsilon_2} \left(\frac{1}{\kappa} C(t)\delta(t) + D(t) \right) dt \geq \frac{1}{\kappa} \underline{C} \delta_l(\varepsilon_B)(\varepsilon_2 - \varepsilon_B). \tag{47}$$

Thus, inserting (46) into (47), we have

$$\varepsilon_2 - \varepsilon_B \leq \frac{-\dot{x}_A(\varepsilon_B)}{\frac{\underline{C}\eta_1}{\overline{M}_1}(\frac{1}{2}(\frac{2M_2\omega_r}{\overline{P}\eta_2}\Delta\dot{\theta})^{\sqrt{M_1/M_2}} - 1)}. \tag{48}$$

We know that $\omega_r \propto \sqrt{1/\kappa}$ and $0 < \sqrt{M_1/M_2} < 1$. From (48), we get

$$(\varepsilon_2 - \varepsilon_B) \sim \mathcal{O}\big(\kappa^n\big), \quad 0 < n < 1/2. \tag{49}$$

By (43) and (49), the assumption $A(t) \in \mathcal{D}(A)$ previously prescribed is guaranteed automatically. Thus, we can confirm that $\dot{x}_A(t_s) = 0$ is an unavoidable event that must appear in the rod dynamics as κ goes to zero.

Summarizing the time-scale analysis presented in this section, let us give a conclusion as follows:

When the rod dynamics is initialized in the inconsistent mode with $A(t_0) < 0$ and $B(t_0) < 0$, there exists a crucial contact parameter κ^{**} ($\kappa^{**} = \min(\kappa^*, \kappa_3)$) such that for all $\kappa < \kappa^{**}$ the motion of the contact point must be brought into a sticking event $\dot{x}_A(t_s) = 0$, where the time t_s is equal to either $\varepsilon_{\dot{x}_A}$ or ε_2.

5 Painlevé paradox related to an impact

As the event $\dot{x}_A(t_s) = 0$ is proved unavoidable, we can prove that an impact must be related to the Painlevé paradox. Generally, an impact corresponds to a rapid dynamics that takes the following characteristics:

1. The time interval for the contact process should converge to zero when the contact stiffness goes to infinity.
2. The normal contact force can rapidly reach a large magnitude that decreases quickly during a short time interval.
3. The impulse of the normal contact force during the short time interval takes a finite value.
4. The configuration of the system can be considered constant if the contact stiffness is large enough.

By the above analysis, as κ goes to zero, we have the results for the system starting from an inconsistent mode to the instant of tangential velocity vanishing, namely $\dot{x}_A(t_s) = 0$:

1. The time interval, $\varepsilon_s = t_s - t_0$, and the variation of the configuration of the system, can be arbitrarily small;see (25), (34), and (49).
2. The normal impulse $I(t_s) = \int_{t_0}^{t_s} \frac{1}{\kappa}\delta(t)\,dt$ is bounded; see (42).
3. The normal force $F_n(t_s) = \delta(t_s)/\kappa$ at the instant when $\dot{x}_A(t_s) = 0$ is divergent with the decrease of κ since $\delta(t_s) \propto \kappa^{(1-n)}$, $0 < n < 1/2$; see (46).

In order to confirm that an impact is truly related to the Painlevé paradox, the normal force should converge to a pulse function. Namely, the normal force starting from the occurrence of the Painlevé paradox can quickly increase to an extremely large amplitude, then

the large amplitude can quickly decrease to zero so that a complete process of an impact finishes. To prove that the subsequent motion of the rod follows this process, we need to investigate the friction status when $\dot{x}_A(t_s) = 0$ occurs.

5.1 Friction status at the instant of tangential velocity vanishing

At the instant $\dot{x}_A(t_s) = 0$, the relationship $F_\tau(t) = \mu F_n(t)$ prescribed to (12) breaks down, and a new relationship should be given by checking whether the horizontal dynamics of the rod motion satisfies a tangential velocity constraint defined as $\dot{x}_A(t) = 0$ (stick status in friction).

By the second equation in (9), together with $\ddot{x}_A(t) = 0$ for friction in a stick state, we get

$$\frac{F_\tau(t)}{F_n(t)} = \frac{3\sin\theta\cos\theta}{1+3\sin^2\theta} - \frac{\dot{\theta}^2\cos\theta}{1+3\sin^2\theta}\frac{1}{F_n(t)}. \tag{50}$$

At time t_s, we know that $A(t_s) \in \mathcal{D}(A)$ and $C(t_s) > 0$ when the value of κ is limited in a range $\kappa < \kappa^{**}$. Using $C(t) = (\mu + 3\sin\theta(-\cos\theta + \mu\sin\theta)) > 0$, we get

$$0 < \frac{3\sin\theta\cos\theta}{1+3\sin^2\theta} < \mu. \tag{51}$$

Note that the second term in (50) is always negative. Together with the inequality in (51), Eq. (50) means that the condition, $0 < F_\tau(t_s)/F_n(t_s) < \mu$, must exist at time t_s. Namely, the rod must enter into a stick status once the tangential velocity $\dot{x}_A(t)$ vanishes at the instant t_s.

5.2 Dynamics of the rod in a stick status

Although a stick status exists at time t_s, we cannot say this status is always retained in the subsequent motion of the rod. Note that the frictional relationship of a stick status, expressed in (50), reveals that the ratio $F_\tau(t)/F_n(t)$ may become negative and its absolute value may be larger than μ_s if $F_n(t)$ is small enough. This means that the sticking motion may end at the occurrence of a reverse-slipping motion.

Suppose that the stick motion at the contact point experiences a time interval $[t_s, \varepsilon_3]$. In order to analyze the rod dynamics during this time interval, we first introduce assumptions as follows:

1. The variation of θ is still limited in the range given by the domain $\mathcal{D}(A)$.
2. The value of $\dot{\theta}(t)$ is bounded.

The first assumption is reasonable since $\varepsilon_A \sim \mathcal{O}(\kappa^0)$, and the second assumption comes to be true if the obtaining value of ε_3 under the above assumptions can be arbitrarily small as $\kappa \to 0$.

During a stick status, the direction of the friction force may change from positive to negative under the velocity constraint $\dot{x}_A(t) = 0$. If a transition from a stick state to a reverse slip state occurs at instant ε_3, there is a condition given by:

$$F_\tau(\varepsilon_3) = -\mu_s F_n(\varepsilon_3), \tag{52}$$

where μ_s is the static coefficient of friction.

Note that (50) still holds at instant ε_3. Combination of (50) and (52) leads to

$$F_n(\varepsilon_3) = \frac{\dot{\theta}^2\cos\theta}{3\sin\theta\cos\theta + \mu_s(1+3\sin^2\theta)}. \tag{53}$$

In terms of $F_n(t) = \delta(t)/\kappa$, we can define a critical normal deformation δ^* responsible for the occurrence of a reverse slip motion,

$$\delta^* \triangleq \delta(\varepsilon_3) = \frac{\dot{\theta}^2 \cos\theta}{3\sin\theta\cos\theta + \mu_s(1+3\sin^2\theta)}\kappa \sim \mathcal{O}\big(\kappa^1\big). \tag{54}$$

If the stick motion can end to start a reverse slip motion, we must prove that δ^* is accessible by the fast variable $\delta(t)$. Note that friction during sticking always satisfies the relationship given by (50). Substituting it into the first equation in (9), together with $F_n(t) = \delta(t)/\kappa$, gives the governing equation for $\delta(t)$:

$$\ddot{\delta}(t) = -\frac{4}{\kappa(1+3\sin^2\theta)}\delta(t) + 1 - \frac{4\sin\theta}{1+3\sin^2\theta}\dot{\theta}^2. \tag{55}$$

During sticking, it is clear that the boundary-layer dynamics governed by (55) becomes stable since the coefficient before $\delta(t)$ is always negative. Therefore, as κ is small enough, the value of $\dot{\delta}(t)$ will eventually decrease and become negative to make $\delta(t)$ decrease, too. However, no analytic solution can be obtained from (55) due to the coupling with the slow variable θ. In order to prove that $\delta(t)$ in (55) can attain δ^*, let us construct two linear oscillatory systems expressed as follows:

$$\begin{cases} \ddot{\delta}_l^s(t) = -\dfrac{4}{\kappa}\delta_l^s(t) + 1 - 4\dot{\theta}_m^2, \\ \ddot{\delta}_r^s(t) = -\dfrac{1}{\kappa}\delta_r^s(t) + 1, \end{cases} \tag{56}$$

which are obtained from (55), replacing the relevant terms by their upper and lower bounds, where $\dot{\theta}_m$ represents the maximum of the angular velocity $\dot{\theta}$ of the system (55) during $[t_s, \varepsilon_3]$.

Clearly, the two linear systems have stable equilibrium positions given by

$$\bar{\delta}_l^s = \frac{(1-4\dot{\theta}_m^2)\kappa}{4} \sim \mathcal{O}\big(\kappa^1\big), \qquad \bar{\delta}_r^s = \kappa \sim \mathcal{O}\big(\kappa^1\big), \tag{57}$$

which have the same order $\mathcal{O}(\kappa^1)$ as in δ^* in (54). It is worth noting that, if $\bar{\delta}_l^s < 0$, contact has been separated prior to the arrival of the equilibrium position.

Assign the two linear systems in (56) to start their motions from the same initial conditions ($\delta(t_s) > 0$, $\dot{\delta}(t_s) > 0$) as the one of nonlinear system (55). Note that $\delta(t_s) \propto \kappa^{(1-n)}$, $0 < n < 1/2$, see (46) and (49). This means that $\delta(t_s) \gg \delta^* \sim \mathcal{O}(\kappa^1)$. Considering that no energy dissipation exits in the two oscillating systems with stable equilibrium positions near δ^*, we can conclude that the two linear systems must pass through the position δ^* within their half periods. Denote by ε_l and ε_r the time intervals experienced by the left and right systems when they move from position $\delta(t_s)$ to δ^*, respectively. We have

$$\varepsilon_l < \frac{\pi}{2}\sqrt{\kappa} = \mathcal{O}\big(\kappa^{\frac{1}{2}}\big), \qquad \varepsilon_r < \pi\sqrt{\kappa} = \mathcal{O}\big(\kappa^{\frac{1}{2}}\big). \tag{58}$$

In order to prove that the nonlinear system (55) can pass through the position δ^*, let us first compare it with the right linear system in (56) to obtain an error system characterized by $\beta(t) = \delta_r^s(t) - \delta(t)$:

$$\ddot{\beta}(t) + \frac{1}{\kappa}\beta(t) = \frac{1}{\kappa}\frac{3\cos^2\theta}{1+3\sin^2\theta}\delta(t) + \frac{4\sin\theta}{1+3\sin^2\theta}\dot{\theta}^2. \tag{59}$$

Both terms in the right-hand side of (59) are always positive. As the error system starts from the initial state $\beta(t_s) = 0$, $\dot{\beta}(t_s) = 0$, during a half period of the error system, we always have $\beta(t) > 0$ such that $\delta_r^s(t) > \delta(t)$. Namely, the nonlinear system (55) prior to the right linear system, arrives at the position δ^* within a time interval $(\varepsilon_3 - t_s) < \varepsilon_r$.

Similarly, we can compare (55) with the left system in (56) by denoting $\alpha(t) = \delta_l^s(t) - \delta(t)$ to obtain another error system:

$$\ddot{\alpha}(t) + \frac{4}{\kappa}\alpha(t) = -\frac{4}{\kappa}\frac{3\sin^2\theta}{1+3\sin^2\theta}\delta(t) - 4\dot{\theta}_m^2 + \frac{4\sin\theta}{1+3\sin^2\theta}\dot{\theta}^2. \tag{60}$$

The terms of right-hand side of (60) are always negative. Similar to the above analysis, we consequently have $\delta(t) > \delta_l^s(t)$. As the left linear system arrives at the position δ^*, the nonlinear system delays the time to reach that position. Namely, we have $\varepsilon_3 - t_s > \varepsilon_l$.

In summary, the evolution of $\delta(t)$ in the nonlinear system (55) is enveloped by the solutions of the left and right linear oscillating systems, both of which can reach position δ^*. Therefore, it can also be reached by (55). Then we can say the stick motion must end and be transferred into a reverse slip motion. The time of reaching position δ^* is limited in a range as follows:

$$\frac{\pi}{2}\sqrt{\kappa} < \varepsilon_3 - t_s < \pi\sqrt{\kappa} \sim \mathcal{O}\big(\kappa^{\frac{1}{2}}\big). \tag{61}$$

Let us recall the assumptions introduced for the above analysis, namely $A(t) \in \mathcal{D}(A)$ and $\dot{\theta}(t)$ bounded. It is clear that they can be satisfied since $(\varepsilon_3 - t_s)$ takes an arbitrarily small value along with κ.

5.3 Dynamics of the rod in a reverse slip mode

As a reverse slip motion starts, there is a relationship $F_\tau(t) = -\mu F_n(t)$. Substituting it into the first equation in (9), together with $F_n(t) = \delta(t)/\kappa$, we get

$$\ddot{\delta}(t) = -\frac{1}{\kappa}\big(1 + 3\cos\theta(\cos\theta + \mu\sin\theta)\big)\delta(t) + 1 - \dot{\theta}^2\sin\theta. \tag{62}$$

Unlike the first equation in (12), the coefficient of $\delta(t)$ in (62) now becomes negative. Note that the reverse slip motion starts from an initial state $\delta^* > 0$ and $\dot{\delta}^* < 0$. Therefore, the possibility for the evolution of $\delta(t)$ in a reverse slip motion is that its value will decrease further and the absolute value of $\dot{\delta}(t)$ will increase, such that the event $\delta(t_f) = 0$ related to the contact separation can be reached.

Although the reverse-slip mode theoretically exists, it can be neglected when modeling the Painlevé paradox as an impact [28, 30]. This can be explained as follows: By (54) for δ^* and $F_n(\varepsilon_3) = \delta(\varepsilon_3)/\kappa$, it is clear that the small parameter is eliminated from the expression of the normal contact force $F_n(\varepsilon_3)$. This means that the value of the contact force at the end of the stick motion has been resumed into a bounded value at the level near to gravity, thus we can approximately consider that an impact process finishes at the end of the stick motion.

5.4 Summary of the qualitative analysis

Based on the qualitative analysis for a sliding rod in Painlevé paradox, we can conclude that an impact initialized with zero normal velocity must occur if the contact interface is hard enough. This impact is basically made of three kinds of periods: An initial period of sliding, a period of sticking, and a reverse slip phase. In order to clarify the above developments,

Table 1 Time scales and the variation of the coefficients following the chronological order of the three frictional statuses

Frictional status	Time scales		Boundary-layer: $\ddot{\delta}(t) = (\cdot)\delta(t) + \cdots$
	Start time	End time	$(\cdot)$
Left-sliding	$t_0 = 0$	$t_s = \varepsilon_{\dot{x}_A}$ (see (34)) or $t_s = \varepsilon_2$ (see (40) and (49))	$-\frac{1}{\kappa}A(t) > 0$ in (12)
Sticking	t_s	ε_3 (see (61))	$-\frac{4}{\kappa(1+3\sin^2\theta)} < 0$ in (55)
Reverse-sliding	ε_3	t_f	$-(1 + 3\cos\theta(\cos\theta + \mu\sin\theta))/\kappa < 0$ in (62)

Table 1 presents the evolution of the boundary-layer dynamics and the time scales, following the chronological order of the three frictional statuses.

One can use Table 1 to roughly explain why the Painlevé paradox can result in a tangential impact. The unstable boundary layer during the left-sliding mode has an ability of making the contact point dig into the contact surface, such that certain potential energy, scaled by $\delta(t)$ in our analysis, will be accumulated into the contact surface. The energy accumulation accompanies energy dissipation by friction to decrease the slip velocity. Once the slip velocity vanishes, the boundary layer in a stick mode becomes stable, and the energy within the boundary layer will be released to push the contact point depart from the contact surface. Namely, after the inconsistent mode has been escaped with a tangential impact, the rod detaches from the unilateral constraint. This means that the system does not enter the indeterminant mode, when initialized in the inconsistent mode [5].

6 Conclusions and discussions

In this paper, the existence of a tangential impact for the Painlevé paradox is analyzed. By a compliance-based model, we successfully prove that the Painlevé paradox in the inconsistent case truly results in an impact that occurs in a specific scenario without any initial normal velocity.

The process in our proof is based on a time scale analysis that is performed using a differential comparison theorem to consider the possible events induced by the peculiar property of Coulomb's friction law. By taking the contact stiffness as an adjustable parameter, we express the time scales related to different events as functions with respect to the contact stiffness, then compare their values to detail the dynamics process. As the contact stiffness goes to infinity, we successfully exhibit that the dynamics in the Painlevé paradox takes all the characteristics of an impact.

Generally, the problem of the Painlevé's paradox represents a class of systems of which the ordinary differential equations are not stable on the manifold defined by the constraint equations. From the perspective of mathematics, this problem belongs to a singularity that cannot allow its global approximate solutions to be constructed using singular perturbation techniques. Nevertheless, nature rejects any singularity, and always selects new physical mechanisms to adjust its dynamic responses. For the problem of the Painlevé's paradox in mechanical systems, the mechanism comes from the discontinuity property of dry friction. The study of the problem of Painlevé paradox has a scientific implication in the understanding of the mathematical properties of nonlinear ordinary differential systems subject to *unilateral constraints*, and also play a practical role in discovering the physical mechanism underlying a variety of instability phenomena of mechanical systems.

Acknowledgements The authors would like to acknowledge the anonymous reviewers for their detailed, valuable, and constructive comments, which definitely contribute to the improvement of the paper. This work was supported by the Natural Science Foundation of China (11172019, 11132001, 11472011) and 'Fanzhou' Youth Research Foundation (20110501).

References

1. Painlevé, P.: Sur les lois du frottement de glissement. C. R. Hebd. Séances Acad. Sci. **121**, 112–115 (1895)
2. Moreau, J.J.: Unilaterial contact and fry friction in finite freedom dynamics. In: Nonsmooth Mechanics and Applications, pp. 1–82. Springer, Vienna (1988)
3. Lötstedt, P.: Mechanical systems of rigid bodies subject to unilateral constraints. SIAM J. Appl. Math. **42**, 281–296 (1982)
4. Stewart, D.E.: Rigid-body dynamics with friction and impact. SIAM Rev. **42**(1), 3–39 (2000)
5. Brogliato, B.: Nonsmooth Mechanics, 2nd edn. Springer, London (1999)
6. Lecornu, L.: Sur le frottement de glissement. C. R. Acad. Sci. **140**, 635–637 (1905)
7. Mandel, J.: Cours de Mécanique. École Polytechnique (1951)
8. Dupont, P.E., Yamajako, S.P.: Stability of frictional contact in constrained rigid-body dynamics. IEEE Trans. Robot. Autom. **13**(2), 230–236 (1997)
9. Song, P., Pang, J.S., Kumar, R.V.: A semi-implicit time-stepping model for frictional compliant contact problems. Int. J. Numer. Methods Eng. **60**, 2231–2261 (2004)
10. Song, P., Dupont, P., Kraus, P., Kumar, V.: Analysis of rigid-body dynamic models for simulation of systems with frictional contacts. J. Appl. Mech. **68**(1), 118–128 (2001)
11. Anitescu, M., Potra, F.A.: Time-stepping schemes for stiff multi-rigid-body dynamics with contact and friction. Int. J. Numer. Methods Eng. **55**(7), 753–784 (2002)
12. Zhao, Z., Chen, B., Liu, C.: Impact model resolution on Painlevé's paradox. Acta Mech. Sin. **20**(6), 659–660 (2004)
13. Shen, Y., Stronge, W.J.: Painlevé paradox during oblique impact with friction. Eur. J. Mech. A, Solids **30**, 457–467 (2011)
14. Kane, T.R., Levinson, D.A.: Dynamics: Theory and Applications. McGraw-Hill, New York (1985)
15. Grigoryan, S.S.: The solution to the Painleve paradox for dry friction. Dokl. Phys. **46**(7), 499–503 (2001)
16. Ben-David, O., Rubinstein, S.M., Fineberg, J.: Slip-stick and the evolution of frictional strength. Nature **463**, 76–79 (2010)
17. Baraff, D.: Coping with friction for non-penetrating rigid body simulation. Comput. Graph. **25**(4), 31–40 (1991)
18. Génot, F., Brogliato, B.: New results on Painlevé paradoxes. Eur. J. Mech. A, Solids **18**, 653–677 (1999)
19. Ivanov, A.P.: Singularities in the dynamics of systems with non-ideal constraints. J. Appl. Math. Mech. **67**(2), 185–192 (2003)
20. Payr, M., Glocker, C.: Oblique frictional impact of a bar: analysis and comparison of different impact laws. Nonlinear Dyn. **41**, 361–383 (2005)
21. Mamaev, I.S., Ivanova, T.B.: The Dynamics of a rigid Body with a sharp edge in contact with an inclined surface in the presence of dry friction. Regul. Chaotic Dyn. **19**(1), 116–139 (2014)
22. Zhao, Z., Liu, C., Chen, B.: The Painlevé paradox studied at a 3D slender rod. Multibody Syst. Dyn. **19**, 323–343 (2008)
23. Pfeiffer, F., Glocker, C.: Multibody Dynamics with Unilateral Contacts. Wiley, New York (1996)
24. Stewart, D.E., Trinkle, J.: An implicit time-stepping scheme for rigid body dynamics with inelastic collisions and coulomb friction. Int. J. Numer. Methods Eng. **39**, 2673–2691 (1996)
25. Anitescu, M., Potra, F.A., Stewart, D.: Time-stepping for three-dimensional rigid-body dynamics. Comput. Methods Appl. Mech. Eng. **177**, 183–197 (1999)
26. Brogliato, B., ten Dam, A.A., Paoli, L., Génot, F., Abadie, M.: Numerical simulation of finite dimensional multibody nonsmooth dynamical systems. ASME Appl. Mech. Rev. **55**(2), 107–150 (2002)
27. Hurmuzlu, Y., Génot, F., Brogliato, B.: Modeling, stability and control of biped robots—a general framework. Automatica **40**, 1647–1664 (2004)
28. Zhao, Z., Liu, C., Ma, W., Chen, B.: Experimental investigation of the Painlevé Paradox in a robotic system. ASME J. Appl. Mech. **75**, 041006 (2008)
29. Leine, R.I., Brogliato, B., Nijmeijer, H.: Periodic motion and bifurcations induced by the Painlevé paradox. Eur. J. Mech. A, Solids **21**, 869–896 (2002)
30. Liu, C., Zhao, Z., Chen, B.: The bouncing motion appearing in a robotic system with unilateral constraint. Nonlinear Dyn. **49**, 217–232 (2007)

31. Or, Y., Rimon, E.: Investigation of Painlevé's paradox and dynamic jamming during mechanism sliding motion. Nonlinear Dyn. **67**(2), 1647–1668 (2012)
32. Or, Y.: Painlevé's paradox and dynamic jamming in simple models of passive dynamic walking. Regul. Chaotic Dyn. **19**(1), 64–80 (2014)
33. Nordmark, A., Dankowicz, H., Champneys, A.: Friction-induced reverse chatter in rigid-body mechanisms with impacts. IMA J. Appl. Math. **76**(1), 85–119 (2011)
34. Stewart, D.E.: Convergence of a time-stepping scheme for rigid-body dynamics and resolution of Painlevé's problem. Arch. Ration. Mech. Anal. **145**, 215–260 (1998)
35. Nordmark, A., Dankowicz, H., Champneys, A.: Discontinuity-induced bifurcations in systems with impacts and friction: discontinuities in the impact law. Int. J. Non-Linear Mech. **44**, 1011–1023 (2009)
36. Brach, R.M.: Impact coefficients and tangential impacts. ASME J. Appl. Mech. **64**, 1014–1016 (1997)
37. Le Suan, A.: The Painlevé paradoxes and the law of motion of mechanical systems with Coulomb friction. J. Appl. Math. Mech. **54**(4), 430–438 (1990)
38. Liu, C., Zhang, H., Zhao, Z., Brogliato, B.: Impact-contact dynamics in a disc-ball system. Proc. R. Soc. A **469**, 20120741 (2013)
39. Walter, W.: Differential inequalities and maximum principles: theory, new methods and applications. Nonlinear Anal. Theory Methods Appl. **30**(8), 4695–4711 (1997)